Research Article

Emad Ali, Mohamed K. Hadj-Kali*, Salim Mokraoui, Rawaiz Khan, Meshal Aldawsari, and Mourad Boumaza

Exergy analysis of a conceptual CO_2 capture process with an amine-based DES

Abstract: The energy efficiency of an absorption–desorption system for carbon dioxide capture from flue gas utilizing methyltriphenylphosphonium bromide-monoethanolamine (MEA) deep eutectic solvent is investigated in this article. According to the results, when the working pressure of the absorber column increases, the process becomes significantly exergy deficient, with an exergy loss of 7.63 MW compared to 5.7 MW for a normal MEA process. The majority of the exergy deficit is due to flue gas compression effort, which accounts for 99% of the total process exergy. The process's exergy shortfall can be improved by lowering the absorber pressure from 10 to 3 atm, lowering the carbon dioxide removal efficiency from 90% to 60%, and increasing the solvent-to-gas ratio from 075 to 7.05. Furthermore, the incorporation of an energy recovery device could allow for an 80–90% reduction in the energy consumed by the gas compressor when running at 10 atm, from 5.7 to 1.2 MJ·kg CO_2^{-1}. With this adjustment, the deep eutectic solvent-based process can match or outperform the corresponding aqueous alkanolamine solvent-based process in terms of exergy destruction and specific energy consumption.

Keywords: deep eutectic solvents, CO_2 capture, exergy analysis, energy recovery

Abbreviations

C_p	heat capacity (kJ·kg^{-1}·K^{-1})
E	exergy (kJ·kg^{-1})
G	sour gas flow rate (kmol·h^{-1})
H, H_0	enthalpy and reference enthalpy (kJ·kg^{-1})
L	solvent circulation rate (kmol·h^{-1})
m	mass flow rate (kg·s^{-1})
M_w	molecular weight (g·mol^{-1})
mHE2	heating fluid flow rate in heat exchanger 2 (kg·kg CO_2^{-1})
mHE3	cooling fluid flow rate in heat exchanger 3 (kg·kg CO_2^{-1})
mHE4	cooling fluid flow rate in heat exchanger 4 (kg·kg CO_2^{-1})
mCon	coolant flow rate in stripper condenser (kg·kg CO_2^{-1})
mReS	steam flow rate in reboiler (kg·kg CO_2^{-1})
P	pressure (atm)
P_0	reference pressure (atm)
P_r	reduced pressure
P_a	absorber pressure (atm)
Q	heat load (kJ·s^{-1})
R	ideal gas constant
S, S_0	entropy, reference entropy (kJ·kg^{-1}·K^{-1})
T_0	reference temperature (K)
T	temperature (K)
T_a	absorber temperature (K)
T_c	critical temperature (K)
T_n	normal boiling temperature (K)
T_r	reduced temperature
T_s	stripper temperature for DES process (K)
THE2$_i$, THE2	inlet, outlet temperature of heating fluid in HE2 (K)
THE3$_i$, THE3	inlet, outlet temperature of heating fluid in HE3 (K)
THE4$_i$, THE4	inlet, outlet temperature of heating fluid in HE4 (K)
T_{st}	stripper top temperature (K)
T_{sd}	stripper distillate temperature (K)

* **Corresponding author: Mohamed K. Hadj-Kali,** Chemical Engineering Department, College of Engineering, King Saud University, PO Box 800, Riyadh 11421, Saudi Arabia, e-mail: mhadjkali@ksu.edu.sa
Emad Ali, Salim Mokraoui, Rawaiz Khan, Meshal Aldawsari, Mourad Boumaza: Chemical Engineering Department, College of Engineering, King Saud University, PO Box 800, Riyadh 11421, Saudi Arabia

T_{re}	stripper reboiler temperature (K)
T_{si}	stripper inlet temperature (K)
T_{sb}	stripper bottom temperature (K)
W	work $(kJ \cdot s^{-1})$
x_f, x_o	CO_2 mole fraction in a lean and rich solvent, respectively

Greek letter

ω	the acentric factor
η_p	pump efficiency
η_c	compressor efficiency
γ	the heat capacity ratio

Subscript

i, in	input
o, out	output
0	reference

Superscript

L	liquid
R	residual
V	vapor

1 Introduction

Globally, energy-intensive activities are the primary sources of anthropogenic carbon dioxide (CO_2) emissions, with fossil fuel combustion in transportation, power production, and industry accounting for around 90% of total emissions [1]. After 3 years of stagnant or little global emissions between 2014 and 2016 [2,3], CO_2 emissions rose by 1.6% in 2017 to 36.2 Gt (billion tons) and grew a further 2.7% in 2018 (range: 1.8–3.7%) to a record of 37.1 ± 2 Gt CO_2 [4]. According to the International Energy Agency (IEA), due to the increasing energy demand, global CO_2 emissions from the energy-producing sector increased by 1.7% in 2018, reaching a historic high of 33.1 Gt CO_2, the fastest pace of rise since 2013. Although the emissions from all fossil fuels increased, the power sector alone contributed nearly two-thirds of the emissions growth. Specifically, coal-based power plants alone accounted for more than 10 Gt CO_2. CO_2 is the primary contributor to global warming impacts along with other greenhouse gases [5,6]. CO_2 capture and

storage (CCS) technologies could be a potential solution to mitigate the emission of CO_2 into the atmosphere by up to 20%. However, the debate regarding CCS becomes intense regarding the cost of energy production because it increases by approximately 30–80% when CCS is applied [6,7]. Therefore, for cleaner energy production, it is important to use cost-effective technology.

The conventional CCS approach is CO_2 absorption using liquid absorbents and is considered the most mature, practically operational, and successfully demonstrated technology [8,9]. Considering the techno-economic aspect of the CO_2 chemisorption process, the selection of solvents is decisive. Solvents with fast kinetics of CO_2 absorption, high CO_2 capture capacity, low vapor pressure, and high stability against thermal and oxidative degradation should be ideal for CO_2 capture [10]. Among the liquid solvents, the aqueous alkanolamine solutions such as monoethanolamine (MEA), diethanolamine (DEA), methyl diethanolamine (MDEA), triethanolamine, 2-amino-2-methyl-1-propanol (AMP), and 2-methylaminoethanol were the most commonly used solvents over the last 60 years [11,12]. New amine-based solvents such as dimethylamino-2-methyl-1-propanol [13] and aqueous blends of conventional amines [14] were tested as well. The aqueous blends of MEA, MDEA, and AMP investigated by Chen et al. [14] resulted in a desorption rate up to five times higher than the commercial aqueous 5 M MEA solution, combined with a significantly lower relative heat duty for regeneration and lower operating cost. However, despite the high affinity of amine solvents for CO_2 molecules, some serious technological drawbacks exist when using the conventional aqueous amine scrubbing process. Specifically, the high-energy requirement for absorbent regeneration and the significant equipment corrosion that occurs makes the process challenging and expensive because of the high-temperature difference between CO_2 absorption (50°C) and desorption (120–140°C) units. Therefore, a high amount of energy is required to maintain the thermal difference in this system.

Currently, the critical limitation preventing the implementation of large-scale CCS globally on the major sources of CO_2 emissions is approximately 3.2–4.0 GJ·ton CO_2^{-1}. Through extensive fundamental studies and several industrial demonstrations (e.g., Boundary Dam, Canada, and Petra Nova, USA) [15], using amine-based technologies achieved a great reduction in energy requirements, with 2.3–2.4 GJ·ton CO_2^{-1} removed compared with 3.5 GJ·ton CO_2^{-1} removed with first-generation amine scrubbing [16]. However, the current energy penalty level of CO_2 chemisorption is still unbearable if a full-scale CO_2 removal process is to be implemented for a coal-fired power plant. Researchers focus on exploring refined techniques or

finding new and more efficient amine solutions that could reduce the energy penalty during the regeneration part of the process [17–19]. It has been reported that water might not be the optimal solvent to use due to high heat capacity, the heat of vaporization, and vapor pressure [20], inclusive of high-energy requirements during the regeneration process [21]. Furthermore, the detrimental ability of water to induce the degradation/corrosion of the amine and process equipment is also a concern [22].

Nonaqueous solutions were proposed as possible alternatives, replacing water with room-temperature ionic liquids (ILs), CO_2-binding liquids, or organic solvents such as methanol or ethanol to reduce the energy penalty during the regeneration step [23–27]. The emergence of binary or ternary blended solvents of amines [28,29] or amines with organics [30], such as alcohols, ethers, and glycols, allowed for the design of advanced nonaqueous absorbents. Because of their lower specific heat than water and low desorption temperature, organic solvents could provide significant advantages for saving the regeneration energy and reducing corrosiveness and degradation. In a nonaqueous process using MEA/methanol as an absorbent, the removal of methanol below 373 K for solvent regeneration resulted in enormous energy savings [31]. A mixture of a nonaqueous absorbent of piperazine (PZ) with diethylene glycol to capture CO_2 in a rotating packed bed has been proposed elsewhere [32]. The results showed that using glycols as solvents significantly reduced energy consumption with almost negligible solvent evaporation and avoidance of thermal degradation. Another study demonstrated secondary alkanolamines/EG as cost-effective absorbents for rapid and reversible CO_2 capture [33]. Chen et al. studied the solubility of CO_2 in N-ethylmonoethanolamine solutions using the vapor–liquid equilibrium (VLE) and the absorption–desorption apparatus. Their results showed that the tertiary amine, N,N-diethylethanolamine, used as a nonaqueous solvent demonstrated more excellent performance than alcohols and glycols [34]. Recently, nonaqueous binary absorbents of conventional amines (MEA and MDEA) with low-viscosity ILs were investigated for CO_2 capture. The mixed absorbent MDEA + [BEIM]BF4 with low viscosity demonstrated a high recycling CO_2 capacity, energy-saving capacity, and good renewability [35]. The absorption–desorption performance of CO_2 into several blends of MEA or DEA with glycol ethers (2-methoxy ethanol (2ME) and 2-ethoxy ethanol (2EE)) as nonaqueous solvents has been reported at ambient pressure. It was found that the mixture of MEA and 2ME or 2EE demonstrated a significant reduction in energy consumption (55%) compared with the benchmark aqueous 5.0 M MEA system.

ILs and deep eutectic solvents (DESs) are among the most attractive substitutes that have been examined over the past few years because of their favorable properties. These properties include negligible vapor pressure, high thermal stability, nonflammability, and tuneability for the desired separation process by changing the combination of cations and anions [36]. For CO_2 capture, various ILs containing amine-functionalized cations/anions [35,37], amino acids [38], aprotic heterocyclic anions, super bases [39], and pyridinium anions [40] have been investigated. Nevertheless, the main problems associated with ILs regarding their application for CO_2 capture are their high susceptibility to contamination, poor biodegradability, high toxicity [8], increasing viscosity during CO_2 capture, and high cost for large-scale industrial application [41].

To overcome the problems associated with ILs while retaining their advantages, DESs appeared as a credible alternative [42,43]. DESs are sustainable solvents analogous to ILs but with several advantages over ILs such as biodegradability, high thermal and chemical stabilities, nonflammability, a wide liquid range, and high purity. Furthermore, DESs are less expensive and easier to synthesize by combining an organic halide salt (considered the hydrogen bond acceptor) with another hydrogen bond donor, such as an amine, amide, carboxylic acid, and alcohol in a certain ratio, resulting in the formation of a low melting-temperature solution by using hydrogen bonding interactions [44]. However, despite the significant efforts of researchers in developing novel solvents with outstanding performance regarding CO_2 absorption capacity and low-energy requirements for solvent regeneration, the implementation of these advanced solvents has not yet reached the commercial level, and more efforts are required to test their practical and economic viability on a large scale.

Furthermore, rigorous rate-based models are indispensable for the design, scale-up, optimization, and analysis of the CO_2 absorption/desorption processes inside packed columns [45]. Many researchers have used the ASPEN Plus simulator to analyze and optimize the CO_2 capture process [12,46–48]. Abu-Zahra et al. implemented the ASPEN PlusRadFrac subroutine model to simulate and optimize the energy required for lean solvent regeneration during the CO_2 capture process from a bituminous coal-fired plant. When using a 40 wt% MEA solution and a stripper operating pressure of 210 kPa, the obtained value was 3.0 GJ·ton CO_2^{-1}, which is 23% lower than the base case of 3.9 GJ·ton CO_2^{-1} with MEA [46]. Li et al. recently used ASPEN Plus to develop a rate-based model for CO_2 capture by using the aqueous MEA absorption process from flue gas [47]. The model was systematically studied for process modification (absorber intercooling, rich-split,

and stripper interheating) and the optimization of various parameters (MEA concentration, lean CO_2 loading, lean temperature, and stripper pressure). The minimum regeneration energy obtained from the model was 3.1 MJ·kg CO_2^{-1}, whereas the highest reported value for the reboiler duty is 5.8 MJ·kg CO_2^{-1} [49]. Oh et al. [50] conducted a recent study based on minimizing the energy expenditure of the CO_2 capture process using aqueous MEA. The authors used the UniSim® process simulator to perform four different types of structural process modifications, including flue gas splitting, multiple solvent feeding, and split-stream/semi-lean and absorber inter-cooling. They inferred that the minimum energy costs could be attained by applying a combination of all four types of structural modifications. However, significant reductions in energy cost could be achieved by implementing single-process modifications, specifically by splitting the flue gas and feeding it at two different locations in the column.

It is believed that the second-generation amine system performs better in energy savings than the traditional MEA chemical absorption process. Zhang et al. presented a systemic study on the modeling and process analysis of the CO_2 capture process with an AMP + PZ aqueous solvent [51]. Their results revealed that by lowering the CO_2 removal rate, increasing the ratio of AMP in the solvent, and increasing the stripper pressure, the reboiler duty could be reduced. The authors applied various process configuration modifications, including intercooled absorber (ICA), lean vapor compressor (LVC), and rich solvent split (RSS), reducing the energy consumption by 6.7%, 2.7%, and 8.5%, respectively. However, the combination of ICA + RSS + LVC decreased the energy demand by 15.2%. Another group of researchers performed a scale experiment via the process development unit for CO_2 removal from a gas mixture by applying MEA and AMP promoted with PZ. Their findings revealed that using AMP/PZ enables the reduction of the solvent heat duty.

Our group investigated the solubility of CO_2 in different DESs at a moderate pressure of 10 atm [52]. The study showed promising results and promoted using methyltriphenylphosphonium bromide (MTPB)-MEA DES for CO_2 capture from power plant exhaust gases. The model developed based on these results could determine the required solvent circulation rates, CO_2 loadings, and flashing temperatures for specific CO_2 recovery rates and given flue gas conditions [53]. The main objective of this work is to quantify the energy requirements of a DES-based CO_2 capture process and determine the source of the energy losses by performing an exergy analysis. The results are benchmarked against the well-established MEA process.

2 Process description and analysis

A schematic flow sheet of the CO_2 capture process is shown in Figure 1. The process is a combination of an absorber and a stripper column. In the absorber, a lean sorbent is used to remove the CO_2 associated with the sour gas in a 40-stage column. The spent sorbent is regenerated in the stripper, where the exact amount of captured CO_2 is released with the top product. The regenerated solvent is recycled back into the absorber. In this work, the stripper is treated as an atmospheric flash drum where the amount of CO_2 to be released occurs at specific VLE conditions. The baseline operating conditions for this process are listed in Table 1. These data are selected based on our previous work [53] and are in the range used in literature [49]. We assumed that only CO_2 is miscible in the solvent (MTPB-MEA DES), the liquid species transferred to the gas phase are insignificant, the CO_2 absorption is only because of physical interactions, and no chemical reactions occur.

Indeed, as shown in our previous work [52], samples of the DES before and after the absorption of the CO_2 were analyzed using high-performance liquid chromatography (HPLC) and the results showed that only 10% of the amine reacted with the CO_2, while for the aqueous solution of MEA, all of the amines reacted with the CO_2. On the other hand, the detailed design equations and solution methodology of the process are given in our previous work [53]. The numerical solution for the baseline conditions is shown in Figure 1.

In the classical MEA process, the reboiler temperature is limited to 120°C because of the amine thermal instability above this temperature [54]. However, to evaluate the thermal stability of the DES used in this work, we performed a thermogravimetric analysis (TGA) under a nitrogen atmosphere using a Mettler Toledo TGA/DSC instrument. The results obtained are provided as supporting material (Figure A1 in Appendix). This analysis indicates two decomposition temperatures: one corresponding to the decomposition of MEA (at about 150°C) and the other corresponding to the decomposition of MTPB at a much higher temperature (at about 400°C). Therefore, the CO_2 capturing process that runs with this solvent could operate at a higher temperature than the classical MEA aqueous process.

Table 2 lists the process performance at different selected operating pressures for the absorber column. The required liquid sorbent, the lean and rich solvent loadings, and the necessary stripping temperature are estimated at each operating pressure. The results in Table 2 form the baseline for the intended exergy
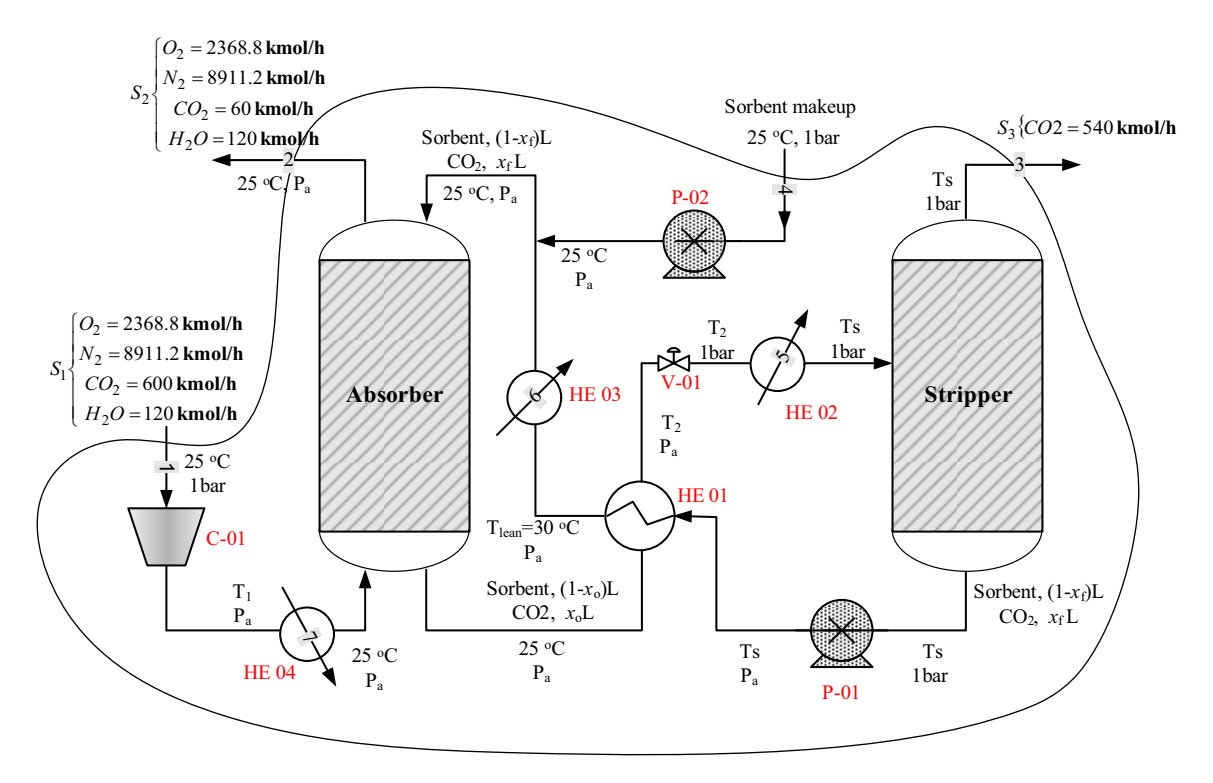
Figure 1: Schematic of CO$_2$ capture process using DES.

analysis. Figure 2 illustrates the process performance with variable absorber pressures. The required solvent amount increases dramatically at low absorber vessel pressures because, at low pressure, the solubility of CO$_2$ in the DES diminishes. Therefore, an additional quantity of solvent is needed to achieve an exact recovery rate of 90%. Similarly, Figure 2 demonstrates how the stripping temperature necessary for separating the captured CO$_2$ from the spent sorbent lowers with pressure. The stripping temperature increases because of the amplification in the solvent circulation rate. Consequently, the rich loading decreases, and a much deeper lean is necessary, demanding additional energy to release the captured CO$_2$.

Our simulation indicates that 90% of the CO$_2$ recovery cannot be achieved by using DES at an absorber pressure of less than 2.2 atm. Furthermore, the simulation results revealed that the process operation below 7 atm is not physically acceptable because the required flashing temperature is beyond the boiling point of the applied DES. Therefore, the simulation was repeated, incorporating a flashing temperature constraint. Table 3 and Figure 2b show the results. The simulation results when operating

Table 1: Baseline operating condition for the CO$_2$ capture process [53]

Gas feed rate (kmol·h^{-1})	12,000
CO$_2$ content (%)	5
H$_2$O content (%)	1
Stripper operating pressure (atm)	1
Number of stages in the absorber	40

Table 2: The performance of CO$_2$ capture process at selected absorber pressure values with 90% recovery

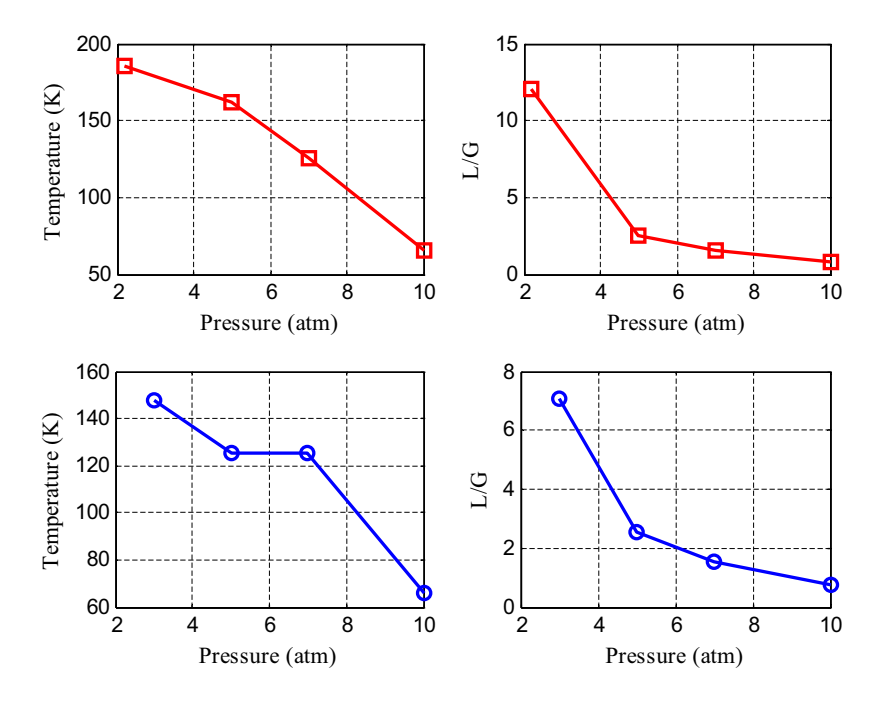| P (atm)	x_f	x_o	L/G	L (kmol·h^{-1})	T_s (°C)	Stream 3		Stream 4 makeup (kmol·h^{-1})
						CO$_2$ (kmol·h^{-1})	DES (kmol·h^{-1})	
10	0.0089	0.0683	0.75	9,015	66	540	2.5	2.5
7	0.0044	0.0332	1.55	18,619	126	540	64.0	64.0
5	0.0022	0.0198	2.55	30,606	162	540	413.1	413.1
2.2	0.0003	0.0041	12.05	144,588	186	540	5,028.9	5,028.9

Figure 2: CO_2 capture process performance at selected values for P_a using DES: squares for 90% recovery and circles for varied recovery.

at a low absorber pressure and a flashing temperature less than the DES boiling point of 155°C are shown in Table 3. At P_a = 5 atm, the recovery must be lowered to 80% or less to ensure a low stripping temperature. Similarly, at P_a = 3 atm, 60% is the maximum allowable recovery that guarantees a stripping temperature below 155°C.

Furthermore, it is found that operating the absorber vessel at a pressure lower than 3 atm does not allow for a flashing temperature less than the boiling point, even at exceptionally low recovery rates.

An absorber column operating at 3 atm is not economically appealing from an energy consumption standpoint because it requires a high stripping temperature. Operating at this low pressure (less than 7 atm) could result in additional costs, such as the cost of materials and pumping. The results in Tables 2 and 3 indicate that the solvent flow rate could reach up to 13 times that required at P_a = 10 atm. Furthermore, the process is operating at a lower recovery rate. Notably, although the process efficiency at low pressure is unappealing, it will be included in the following exergy analysis for demonstration purposes.

3 Exergy principles

Exergy is defined as the maximum possible reversible work that can be obtained from a system or a process. It is useful to measure and compare the energy efficiency of different processes or a process with different configurations [55,56]. Exergy analysis could identify areas of improvement and indicates the priorities toward efficiency enhancement and optimization, which are essential for the creation of new engineering decisions toward sustainable development.

The general exergy (Ex) expression is given by Eq. 1:

$$Ex = (H - H_0) - T_0(S - S_0), \tag{1}$$

were H_0 and S_0 represent the enthalpy and entropy values, respectively, at the environmental temperature T_0, which is usually equal to 298 K. H and S represent the enthalpy and entropy, respectively, at a specified temperature, T (K).

All the processes involve the conversion and consumption of exergy; thus, high efficiency is critical, implying that the exergy use is managed and effective tools are applied.

Table 3: The performance of CO_2 capture process at low recovery rate

P (atm)	Recovery	x_f	x_o	L/G	L (kmol·h^{-1})	T_s (°C)	Stream 3		Makeup (kmol·h^{-1})
							CO_2 (kmol·h^{-1})	DES (kmol·h^{-1})	
5	80%	0.0044	0.0200	2.55	30,612	125	480	55.83	55.83
3	60%	0.0031	0.0074	7.05	84,624	147	360	124.6	124.6

Although the total energy is always conserved, real process exergy is never balanced because of being irreversible, i.e., exergy destruction always occurs. The exergy destruction, ΔE, indicates possible process improvements. In engineering, different flow diagrams are often used to describe the different exergy flows through a process, enabling the selection of the process presenting the least exergy destruction. Generally, the exergy destruction or loss can be written as follows:

$$\Delta E = \sum m_i E_i - \sum m_0 E_0 - Q\left(1 - \frac{T_0}{T}\right) - W, \quad (2)$$

where m_i and m_0 represent the mass input and output to the system, Q is the heat flow to the system, and W is the workflow to the system.

If the system is adiabatic ($Q = 0$) and does not require any work ($W = 0$), then Eq. 2 becomes Eq. 3:

$$\Delta E = \sum m_i E_i - \sum m_0 E_0. \quad (3)$$

The standard conditions considered in this work are $T_0 = 298$ K and $P_0 = 1$ atm.

4 Enthalpy and entropy change calculations

The estimation of exergy requires calculating the enthalpy and entropy of the fluids involved in the process. For the fluids used in the system, such as water and the liquid solvent, the enthalpy and entropy are functions of the temperature only, which could be calculated using the following equations for constant heat capacity:

$$\Delta H = C_p \Delta T, \quad (4)$$

$$\Delta S = C_p \ln\left(\frac{T}{T_0}\right). \quad (5)$$

For compressible gases at the elevated pressure, the enthalpy can be calculated as follows:

$$\Delta H = H - H_0 = H^R(T, P) + \int_{T_0}^{T} C_p dT - H^R(T_0, P_0), \quad (6)$$

where the residual property can be calculated from the following correlation [49]:

$$\frac{H^R}{RT_C} = P_r\left[\left(0.083 - \frac{1.097}{T_r^{1.6}}\right) + \omega\left(0.139 - \frac{0.894}{T_r^{4.2}}\right)\right]. \quad (7)$$

Similarly, the gas entropy can be found using Eq. 8:

$$\Delta S = S - S_0 = S^R(T, P) + \left(\int_{T_0}^{T} C_p\frac{dT}{T} - R\ln\frac{P}{P_0}\right) \quad (8)$$
$$- S^R(T_0, P_0),$$

$$\frac{S^R}{R} = -P_r\left[\frac{0.675}{T_r^{2.6}} + \omega\frac{0.722}{T_r^{5.2}}\right]. \quad (9)$$

Eqs. 6–9 allow the calculation of enthalpy and entropy changes for any temperature and pressure variation.

The energy required for fluid pumping is calculated using Eq. 10:

$$E = Q\Delta P/\eta_p. \quad (10)$$

In Eq. 10, Q is the volumetric flow rate in cubic meters per second, ΔP is the pressure difference in pascals, and η_p is the pump efficiency. Similarly, the energy required for gas compression can be calculated using Eq. 11:

$$E = m(H_{\text{out}} - H_{\text{in}})/\eta_c, \quad (11)$$

where m is the mass flow rate of the gas, H is the specific enthalpy for the inlet and outlet streams, and η_c is the compressor efficiency.

5 Results and discussion

5.1 Effect of operating conditions for the baseline case

Figure 1 illustrates the CO$_2$ capture flowsheet utilizing the DES solvent, which shows the operating parameters of all streams. The absorber operating pressure (P_a) and stripper working temperature (T_s) are predetermined, as shown in Tables 2 and 3. The temperature of the stream leaving HE01 and entering HE03 is arbitrarily set at 35°C, whereas T_2 is determined using an enthalpy balance around HE01. $T1$, the temperature of the gases exiting the compressor, was computed in the same way using the isentropic compression equation:

$$\frac{T_2}{T_1} = \left(\frac{P_2}{P_1}\right)^{\frac{\gamma-1}{\gamma}}, \quad (12)$$

where γ is the heat capacity ratio equals C_p/C_v. We assume that the temperature change of the liquid solvent during compression through pumps P01 and P02 and expansion through valves V01 and V02 is negligible. Notably, water is used as a cooling medium in HE03

and HE04. The energy balance around each heat exchanger determines the amount of water used by using arbitrarily fixed temperatures for the inlet and outlet water streams. For HE02, hot water is used for heating when the required stripping temperature is less than 100°C. When T_s exceeds 100°C, as shown in Table 2 for different values for P_a, saturated steam is used to heat the rich sorbent stream. The amount of heating water or steam is computed using the energy balance around HE02. The steam temperature and pressure used for the different values of P_a are taken from the steam tables. The temperature of the steam used in HE02 is chosen to be slightly higher than the required stripping temperature at the corresponding P_a, e.g., when T_s = 126°C, steam at 133.6°C is used. The physical properties of the DES used in this work and MEA are provided in supporting material (Table A1 in Appendix). In this work, the pump efficiency is taken at 60%, and the compressor efficiency is considered to be 70%.

Figure 3: Exergy destruction of the CO_2 capture process using DES at selected pressure values.

5.2 Exergy analysis of DES-based CO_2 capture process

After determining all flow rates and operating parameters with DES as the solvent (Table A2), we performed an exergy analysis for the overall process denoted by the dotted boundary in Figure 1. In this case, the exergy analysis included all streams that cross the boundary (streams 1–4). Therefore, Eq. 2 incorporates the contribution of heat exchangers and compressors to overall exergy loss in which case Table 4 and Figure 3 show the results.

Figure 3 shows that the system's exergy destruction to exergy input decreases with operating pressure but increases again at P_a = 10 atm. To achieve a high recovery rate and the lowest exergy losses, the absorber should be operated at P_a = 7 atm. Examining the precise exergy flow in Table 4 can help you understand the exergy trend with
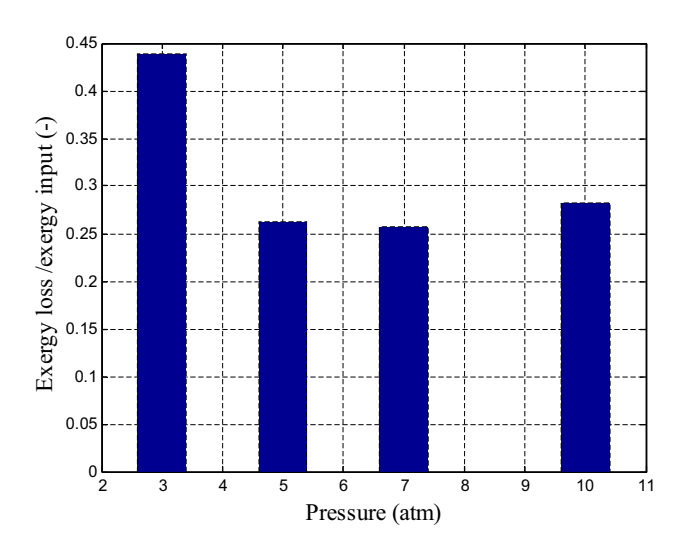
pressure. Because the stripping temperature reaches 148°C at P_a = 3 atm, the thermal energy consumption for heating the rich sorbent in HE2 is the highest. As a result, the equivalent gross exergy loss is the greatest. However, for P_a = 10 atm, the work for compressing the flue gas takes precedence over the stripping energy. The additional compression work raises the net exergy destruction once again. As a result, the compression and heat energies must be balanced. As previously stated, running at low absorber pressures is undesirable due to the increased solvent circulation rate and low CO_2 removal efficiency. Table 4 depicts the exergy flow linked with the process streams. Because of its high pressure, stream 2, the sweetened gas stream, has the largest exergy flow of the other streams. As the pressure decreases, so does the exergy.

It is useful to exploit the large exergy leaving the system by stream 2. The energy consumption when the process is operating at 10 atm (or higher) could be reduced by using the exergy associated with stream 2. This could be

Table 4: Exergy flow and overall exergy loss of CO_2 capture process

Solvent	P_a	T_s	Exergy flow in streams and units										Overall		
			S1	S2	S3	S4	HE2	HE3	HE4	C01	Reb	Cond	Ex_{in}	Ex_{out}	ΔEX
	(atm)	(°C)	(MW)	(MW)	(MW)	(MW)	(MW)	(MW)	(MW)	(MW)	(MW)	(MW)	(MW)	(MW)	(MW)
DES	3	147.8	0.00	8.82	0.26	0.00	6.70	−0.38	−0.35	10.64	—	—	17.33	9.80	7.53
	5	125.2	0.00	12.78	0.15	0.00	1.74	−0.14	−0.55	16.77	—	—	18.51	13.62	4.89
	7	125.6	0.00	15.36	0.18	0.00	0.75	−0.08	−0.70	21.28	—	—	22.03	16.32	5.71
	10	65.6	0.00	18.17	0.02	0.00	0.23	−0.04	−0.87	26.51	—	—	26.75	19.11	7.64
	10 + ERD	65.6	0.00	0.00	0.02	0.00	0.23	−0.04	−0.88	5.25	—	—	5.48	0.94	4.54
MEA	1	40	0.04	0.04	0.018	4×10^{-5}	—	−0.211	—	—	6.26	−0.64	6.5	0.8	5.7

achieved by using a dual-work exchanger energy recovery system. These low-cost energy recovery devices (ERDs) provide greater energy-saving payback and greater operational flexibility for liquids [57,58].

A similar idea is utilized for gases, consisting of a gas turbine (expander) followed by a gas compressor. The power created by the gas turbine is utilized to power the following compressor, which pressurizes another low-pressure gas stream in this device. This device is also known as the gas pressure exchanger or booster, adopting the fundamentals of turbochargers in combustion engines. The so-called ERD for gases is proven useful in industry, for example, in ammonia factories. The purpose of this equipment is to recover energy from the pressurized fluid stream leaving the absorber column. The modified process is shown in Figure 4. Usually, such devices are limited by thermodynamic efficiency; therefore, the pressure of the exiting stream would be less than the inlet pressure of the pressurized stream. For an ERD efficiency of 60%, the pressure of the gas stream exiting the ERD can be 6.3 atm and the corresponding temperature 217°C. In this case, a compressor is still needed to complement the ERD. The main advantage of the modified process is that the purified gas stream exits the process at 1 atm. Consequently, the calculated overall exergy of the modified process is 6.36 MW.

By using the pressure of the exit gas stream with an ERD efficiency of 60%, the process changed from an exergy deficit of 7.64 to 6.36 MW, which is equivalent to a 17% enhancement because the energy recovery in the form of the pressure head within the whole system enhances the conservation of exergy (decrease in exergy loss). If the ERD efficiency can be increased further, the performance of the DES process regarding exergy losses could be enhanced substantially (Table 5). This situation makes the DES-driven CO$_2$ capture process, supported by the energy recovery system, more energy efficient. Usually, the sour gas treated for CO$_2$ removal is the exhaust gas of a power plant. The flue gas leaves the combustion chamber of a power plant at an elevated temperature and pressure (1,494°C and 30 bar, respectively) [59,60]. The immense potential energy of the flue gas is usually used in power plants to produce high-pressure steam. Therefore, the exergy loss due to the compression work can be avoided by integrating the DES-driven CO$_2$ capture process with the power plant.

Table 5: Performance of DES + ERD at 10 atm and different ERD efficiency

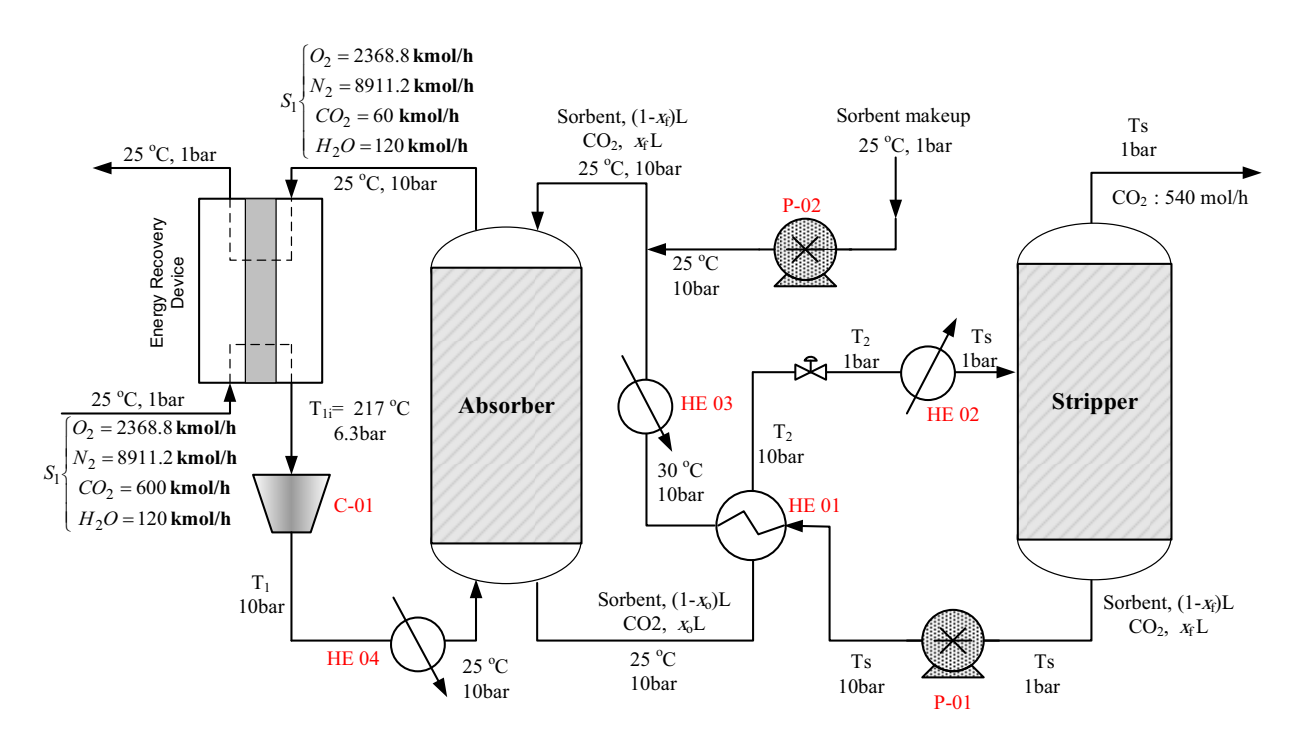| Efficiency (%)	ΔEX (MW)	En (MJ·kg CO$_2^{-1}$)
50	8.370	3.041
60	6.357	2.060
70	4.542	1.400
80	2.884	0.935

Figure 4: Schematic of CO$_2$ capture process using DES with the aid of ERD.

5.3 Energy analysis of DES-based CO_2 capture process

To further analyze the energy requirements of CO_2 capture using DES, the specific energy of each thermal processing unit in the process was analyzed for an absorber operating at 10 and 3 atm. The calculating formulas have been presented in Section 4. The specific energy of captured CO_2, which is a common way to easily compare processes with different capacities or efficiencies, is presented in Table 6. The pump power is the energy required to increase the pressure of the fluid. We neglect the pumping energy required to maintain the circulation rate and to overcome the pressure drop arising from distance, elevation, friction, or equipment. Therefore, the pumping energy for MEA and DES processes is almost null and, thus, is omitted.

The energy consumption of the gas compressor is the highest and can rise to around 6.0 MJ·kg CO_2^{-1} at $P_a = 10$ atm. Consequently, HE04 produces a large amount of energy because it absorbs the compression energy. The compression energy can be reduced by 40% when the pressure is cut to 3 atm. However, at that operating pressure, the specific heating energy of HE02 increases dramatically because of the elevated solvent circulation rate, elevated stripping temperature, and reduced CO_2 recovery. In this case, the total specific energy consumption could be higher at a lower operating pressure. Similarly, the cooling energy of HE03 increases because of the elevated solvent circulation rate and reduced CO_2 recovery. At $P_a = 10$ atm, gas compression consumes the largest energy compared with other units, creating an energy-intensive requirement for CO_2 capture by DES solvents at elevated pressures. At lower operating pressures, the energy demand for compression improves slightly, but the energy needed by HE02 increases substantially because of the excess

Table 6: Units' specific energy requirement for CO_2 capture process

Process unit	DES (3 atm) Energy (MJ· kg CO_2^{-1})	DES (10 atm) Energy (MJ· kg CO_2^{-1})	DES + ERD (10 atm) Energy (MJ· kg CO_2^{-1})	MEA (1 atm) Energy (MJ· kg CO_2^{-1})
C01	3.449	5.735	1.162	—
HE02	4.844	0.238	0.238	—
HE03	−5.253	−0.372	−0.372	−1.57
HE04	−2.431	−4.065	−4.089	—
Reboiler	—	—	—	−2.00
Condenser	—	—	—	5.8

heating requirements from the heating medium, leaving the system with a significant exergy loss.

The net energy requirements sum to 8.3 MJ·kg CO_2^{-1} at $P_a = 3$ atm, compared with 6 MJ·kg CO_2^{-1} at $P_a = 10$ atm. This makes operating at low absorber pressures more energy intensive than operating at a higher pressure. Although coolers HE3 and HE4 provide an abundance of energy suitable for heat integration, their energy cannot be used for heat recovery because the temperature of their corresponding operating streams is much less than T_s. As mentioned earlier, the ERD unit can be incorporated, leading to dramatic energy saving as the specific energy of compression is reduced from 5.74 to 1.16 MJ·kg CO_2^{-1}, and hence, the net energy requirement becomes approximately 1.4 MJ·kg CO_2^{-1}. Furthermore, as shown in Table 5, if ERD devices with an efficiency higher than 60% are available, implementing such a device could make the DES process more efficient regarding exergy destruction and specific energy consumption.

5.4 Exergy analysis of MEA-based CO_2 capture process

For benchmarking purposes, we studied the exergy of the CO_2 capture process using MEA as the solvent. The process flowsheet is depicted in Figure A2. The MEA process has additional reboiler and condenser units. The sorbent preheater (HE02) is not used here because the regenerated solvent stream has sufficient thermal energy to heat the rich solvent stream. In such processes, CO_2 extraction from flue gases is based on chemical absorption. Thus, additional energy is needed to break the reaction bonds and regenerate the solvent. We consider the same CO_2 recovery ratio (90%), flue gas composition and amount, solvent circulation rate, and CO_2 input for a fair comparison with the DES-operated process. The solvent circulation rate and its composition should be recalculated for the MEA-driven process. However, these variables do not affect the overall exergy calculation and are only useful when computing T_{lean}. Table A2 shows the operating conditions of various process streams that are either taken from the literature or fixed at arbitrary values.

The temperature of the liquid stream exiting HE01 and entering HE03 is denoted as T_{lean} and determined by the enthalpy balance around HE01. The enthalpy balance determines the amount of coolant water in HE03 by using a fixed arbitrary temperature for the coolant end-streams. Saturated steam of 130°C will be used in the

reboiler. The reboiler duty is equal to 5.8 MJ·kg CO$_2^{-1}$ and that for the condenser is 2.07 MJ·kg CO$_2^{-1}$ [49]. The necessary physical properties of MEA are presented in Table A1. The reboiler temperature ranges from 90°C to 120°C, with a common value of 120°C [58,59]. The stripper inlet temperature can vary from 75°C to 120°C [59,61–64]. The reported value for the distillate temperature is either 75°C [49,63] or 107°C [56].

For simplicity, the stripper top vapor was set to 100°C to be consistent with the other stripper terminal values. Still, the temperature of the stripper surroundings has a marginal effect on the exergy calculations. For example, T_d has a negligible effect on the exergy analysis because its corresponding flow rate is low, and T_s is only required for estimating T_{lean}. The top and bottom temperatures are not needed because the reboiler and condenser duties are sufficient to conduct the energy analysis. As mentioned earlier, we assume that the effect of compression and expansion of the liquid solvent on the temperature is negligible. The MEA solvent is a 30 wt% water solution. By applying the exergy equations to the CO$_2$ capture process using MEA and on the basis of the aforementioned operating conditions, we obtained an overall exergy destruction of 5.7 MW (Table 4). Note that Table 4 presented negative values, indicating cooling, and, hence, the exergy flow for the corresponding unit will be considered as exergy flowing out of the system boundary. The calculated exergy is somehow subject to the operating conditions used; however, it indicates a better energy efficiency than using DES at P_a = 10 atm and similar energy efficiency when compared with DES operating at 7 atm. When ERD is used, the DES-driven process can be more effective than the MEA method. Furthermore, the exergy input into the MEA process is lost inside the system because it is used to break the chemical reaction bonds to regenerate the solvent. In the DES process, the exergy input via the compressor to pressurize the sour gas enhanced the mass transfer of CO$_2$ and, simultaneously, was transferred to the outlet stream (stream 2). The transferred energy can be further used within the process or further downstream.

5.5 Energy analysis of MEA-based CO$_2$ capture process

The total energy consumption of a typical CO$_2$ capture process is the sum of the thermal energy of regeneration, CO$_2$ product compression, and solvent circulation. The regeneration energy causes a major part of the overall operating cost [65]. Therefore, we consider the reboiler

thermal energy in the MEA process as the baseline for comparison and analysis. Similarly, the compression work in the DES process comprises most of the energy requirements that are equivalent to the reboiler duty in the MEA process. Therefore, operating the DES process at 10 atm requires equivalent specific energy to that of the counterpart MEA process. For example, Øi [59] and Øi and Kvam [66] reported an energy requirement of approximately 3.4 MJ·kg^{-1} CO$_2$ for a CO$_2$ removal of 85%; Abu-Zahra et al. [65] reported an energy consumption in the range of 3.6–4.8 MJ·kg^{-1} CO$_2$ depending on the operating pressure and temperature; Han et al. [63] found that energy consumption of 4.3 MJ·kg CO$_2^{-1}$ resulted in up to 83% recovery, and Mofarahi et al. [49] recorded the highest reboiler duty of 5.8 MJ·kg CO$_2^{-1}$ for CO$_2$ recovery of 89%. Rao and Rubin [67] reported a reboiler heat duty range of 1.6–11 MJ·kg CO$_2^{-1}$ for a recovery range of 41–99.9%.

Another source of energy consumption in DES-based processes is the additional energy for solvent circulation to overcome the pressure drop arising from the viscosity. The viscosity of DES is higher than that of MEA (Table A1). Estimating the increased energy required due to viscosity is difficult since it requires particular design factors such as pipe diameter, length, and elevation. However, we can roughly assume that the additional energy required by DES circulation over that of MEA is proportional to their viscosity ratio, which is approximately 2.4.

5.6 Comparison between MEA and DES processes for small-scale CO$_2$ capture plant

Previous MEA exergy analyses relied on design data, notably the solvent circulation rate and CO$_2$ loading, which are calculated by solving design equations with DES as the solvent. It is worthwhile to review the MEA exergy study based on design data calculated using the MEA solvent. The design data for the MEA method proposed by Li et al. [68] are shown in Table A3. The data provided are sufficient for the overall exergy analysis but not for the unit-by-unit exergy analysis required for the MEA procedure. Notably, in the designated references, the initial feed composition and CO$_2$ loading are reported in grams per gram. To fit our modeling approach, these values are transformed into moles.

For comparison with the DES-driven process, our DES design model will be solved using the given data for the gas flow rate, solvent flow rate, feed composition, and the desired CO$_2$ removal rate to determine the

Table 7: Exergy analysis for the MEA and DES processes

	P_a (atm)	T_a (K)	S1 (kW)	S4 (kW)	S2 (kW)	S3 (kW)	HE2 (kW)	HE3 (kW)	HE4 (kW)	Com (kW)	Re (kW)	Con (kW)	Ex in (kW)	Ex out (kW)	ΔEX (kW)
DES	20	320	0.018	0.000	5.260	0.001	0.247	−0.126	−0.363	12.79	–	–	13.056	5.750	7.31
	15	320	0.018	0.000	4.775	0.006	0.498	−0.126	−0.313	11.09	–	–	11.607	5.220	6.39
	20ERD	320	0.018	0.000	0.017	0.001	0.247	−0.126	−0.032	1,013	–	–	1.277	0.177	1.10
MEA*	1	320	0.018	0.000	0.017	0.000	–	−0.177	–	–	2.083	−0.215	2.101	0.409	1.69

*[68]

stripping temperature and CO_2 loadings. The other necessary operating conditions that are either fixed at arbitrary values or calculated as indicated are listed in Table A4. Notably, our simulation of the DES process indicated that the operating pressure for the absorber must be larger than 10 atm to maintain a stripping temperature below 155°C. For the given low CO_2 content in the flue gas and low CO_2 loadings, controlled by the CO_2 fraction in the outlet sweetened gas, the stripper requires high energy to extract the low CO_2 content from the diluted solvent. After applying the exergy analysis to the MEA and DES processes, the results presented in Table 7 were obtained. The MEA process has much lower exergy destruction than the DES process. Most of the exergy losses in the MEA process originate from the reboiler, whereas, for the DES case, the compression work is the dominant source of exergy destruction. However, when relating the exergy losses to the exergy added to the system, the MEA process becomes inferior to the DES process.

Our DES design model was solved using the given data for the gas flow rate, solvent flow rate, feed composition, and desired CO_2 removal rate to estimate the stripping temperature and CO_2 loadings for comparison with the DES-driven process. Table A4 lists the additional required operating conditions, which are either fixed at arbitrary values or calculated as specified. Notably, our simulation of the DES process revealed that the operating pressure for the absorber must be more than 10 atm to keep the stripping temperature below 155°C. The stripper requires a lot of energy to extract the low CO_2 content from the diluted solvent for the specified low CO_2 content in the flue gas and low CO_2 loadings, which are controlled by the CO_2 percentage in the outlet sweetened gas. The results presented in Table 7 are obtained after applying the exergy analysis to the MEA and DES procedures. The

Table 8: Comparison between the specific energy demand of the MEA and DES processes

Parameter	DES			MEA*
P_a (atm)	20	15	20 + ERD	1
T_s (°C)	60.6	107.7	60.6	120.8
Comp (MJ·kg CO_2^{-1})	31.7	27.5	2.46	—
HE02 (MJ·kg CO_2^{-1})	5.8	5.6	5.80	—
HE03 (MJ·kg CO_2^{-1})	−5.8	−5.8	−5.79	−7.8
HE04 (MJ·kg CO_2^{-1})	−23.2	−20.0	−2.04	—
PE01 (MJ·kg CO_2^{-1})	1.7	1.3	1.73	0
PE02 (MJ·kg CO_2^{-1})	0.0	0.0	0.00	0
Cond (MJ·kg CO_2^{-1})	—	—	—	—
RE01 (MJ·kg CO_2^{-1})	—	—	—	19.01

*[68]

MEA process consumes far less energy than the DES procedure. The reboiler accounts for the majority of exergy losses in the MEA process, whereas the compression work is the primary source of exergy destruction in the DES process. However, when the exergy losses are compared to the exergy added to the system, the MEA process falls short of the DES process.

As previously stated, exergy added to the MEA process is lost within the system, whereas exergy added to the DES process is transferred to the outlet stream in part. As a result, the relocated exergy can be employed further inside the system via pressure recovery units, resulting in increased energy efficiency. Table 8 compares the energy consumption of the MEA and DES procedures. Depending on the operating pressure, the DES process may take up to 34–$38 \, MJ \cdot kg \, CO_2^{-1}$. The MEA system, on the other hand, consumes just $19 \, MJ \cdot kg \, CO_2^{-1}$, providing for 50% of the reduction in energy requirement.

To compete with the MEA-based process in terms of energy usage, the DES-based process should be run at a low absorber pressure. However, while operating at low pressures, our simulation results show a performance constraint in the form of a poor recovery or stripping temperature over the solvent's boiling point. Otherwise, if the benefits of running at greater pressure, such as reduced solvent circulation rate and lower stripping temperature, are desired, an ERD unit can be added to the process. For example, with a 60% ERD, the compression work might be lowered to $0.66 \, MJ \cdot kg \, CO_2^{-1}$ for the baseline scenario and $2.46 \, MJ \cdot kg \, CO_2^{-1}$ for Li et al.'s [68] procedure, representing an 80–90% improvement. Alternatively, the inherited pressure of a power plant's flue gas might be used to replace the compression unit. For highly pressurized sour gases, the DES-based technique is preferred.

6 Conclusions

The energy demand of CO_2 removal from flue gas using amine-based DESs in the absorption–desorption process was investigated in this work. High absorption column pressures are required to provide effective CO_2 physical absorption and, as a result, improved process performance and design requirements. Depending on the processing capacity and operating pressure, the raised pressure increases the exergy deficit to 4–$8 \, MW$ and the energy consumption to roughly 6–$38 \, MJ \cdot kg \, CO_2^{-1}$. We discovered that the main source of exergy shortage is the compression energy of the flue gas. However, when

compared to the MEA-based process, it was found that the DES-based process has a lot better exergy destruction because the exergy inserted is much superior to the exergy lost in the DES process. The energy demand of the MEA process, on the other hand, was discovered to be nearly 50% lower than that of the DES process, where the energy consumption is mostly related to the compression work to the required high pressure. Adding an ERD unit can lower the DES process's energy need by up to 80%. To improve the process economically, we recommend lowering the operating pressure, which reduces exergy loss at the expense of performance. Alternatively, ERDs could be incorporated into the process to reduce compression demand and, as a result, exergy loss. Nonetheless, when applied to contaminated exhaust gases at high pressure, the DES-driven CO_2 capture process could be energy efficient. The study's major goal is to identify a less energy-intensive CO_2 capture technique than the standard MEA solvent. DES solvents are used to alleviate this. However, the suggested DES process necessitates high-pressure operation to maintain the same CO_2 recovery and solvent-to-gas ratios as the standard MEA method, resulting in increased energy consumption owing to flue gas compression. Yet, by employing an ERD, the DES process can outperform the conventional technique. These encouraging findings pave the way for additional research into alternatives to standard MEA solvents.

Author contributions: Emad Ali: conceptualization, writing – original draft, writing – review and editing, and methodology; Mohamed K. Hadj-Kali: conceptualization, formal analysis, writing – review and editing, project administration, and funding; Salim Mokraoui: writing – review and editing and formal analysis; Rawaiz Khan: methodology, writing – review and editing, and visualization; Meshal Aldawsari: resources and writing – review and editing; Mourad Boumaza: methodology, formal analysis, and review.

Conflict of interest: The authors state no conflict of interest.

Data availability statement: All data generated or analyzed during this study are included in this published article and its supplementary information files.

References

[1] Höök M, Tang X. Depletion of fossil fuels and anthropogenic climate change – a review. Energy Policy. 2013;52:797–809.

[2] Jackson RB, Canadell JG, Le Quéré C, Andrew RM, Korsbakken JI, Peters GP, et al. Reaching peak emissions. Nat Clim Change. 2016;6(1):7–10.

[3] Le Quéré C, Andrew RM, Friedlingstein P, Sitch S, Pongratz J, Manning AC, et al. Global carbon budget 2017. Earth Syst Sci Data. 2018;10(1):405–48.

[4] Le Quéré C, Andrew RM, Friedlingstein P, Sitch S, Hauck J, Pongratz J, et al. Global carbon budget 2018. Earth Syst Sci Data. 2018;10(4):2141–94.

[5] Etminan M, Myhre G, Highwood E, Shine K. Radiative forcing of carbon dioxide, methane, and nitrous oxide: A significant revision of the methane radiative forcing. Geophys Res Lett. 2016;43(24):614–2.

[6] Yamasaki A. An overview of CO_2 mitigation options for global warming – emphasizing CO_2 sequestration options. J Chem Eng Jpn. 2003;36(4):361–75.

[7] Budinis S, Krevor S, Dowell NM, Brandon N, Hawkes A. An assessment of CCS costs, barriers and potential. Energy Strategy Rev. 2018;22:61–81.

[8] Mirza NR, Nicholas NJ, Wu Y, Mumford KA, Kentish SE, Stevens GW. Experiments and thermodynamic modeling of the solubility of carbon dioxide in three different deep eutectic solvents (DESs). J Chem Eng Data. 2015;60(11):3246–52.

[9] Molina CT, Bouallou C. Assessment of different methods of CO_2 capture in post-combustion using ammonia as solvent. J Clean Prod. 2015;103:463–8.

[10] Vaidya PD, Kenig EY. CO_2-alkanolamine reaction kinetics: a review of recent studies. Chem Eng Technol. 2007;30(11):1467–74.

[11] Arias AM, Mores PL, Scenna NJ, Mussati SF. Optimal design and sensitivity analysis of post-combustion CO_2 capture process by chemical absorption with amines. J Clean Prod. 2016;115:315–31.

[12] Dinca C. Critical parametric study of circulating fluidized bed combustion with CO2 chemical absorption process using different aqueous alkanolamines. J Clean Prod. 2016;112:1136–49.

[13] Zhang R, He X, Liu T, Li C, Xiao M, Ling H, et al. Thermodynamic studies for improving the prediction of CO_2 equilibrium solubility in aqueous 2-dimethylamino-2-methyl-1-propanol. Sep Purif Technol. 2022;295:121292.

[14] Chen G, Chen G, Peruzzini M, Zhang R, Barzagli F. Understanding the potential benefits of blended ternary amine systems for CO_2 capture processes through 13C NMR speciation study and energy cost analysis. Sep Purif Technol. 2022;291:120939.

[15] Mantripragada HC, Zhai H, Rubin ES. Boundary Dam or Petra Nova – which is a better model for CCS energy supply? Int J Greenh Gas Control. 2019;82:59–68.

[16] Goto K, Yogo K, Higashii T. A review of efficiency penalty in a coal-fired power plant with post-combustion CO_2 capture. Appl Energy. 2013;111:710–20.

[17] Bougie F, Iliuta MC. Sterically hindered amine-based absorbents for the removal of CO_2 from gas streams. J Chem Eng Data. 2012;57(3):635–69.

[18] Novotny V, Vitvarova M, Kolovratnik M, Hrdina Z. Minimizing the energy and economic penalty of CCS power plants through waste heat recovery systems. Energy Procedia. 2017;108:10–7.

[19] Patiño-Echeverri D, Hoppock DC. Reducing the Energy Penalty Costs of Post Combustion CCS Systems with amine-Storage. Environ Sci Technol. 2012;46(2):1243–52.

[20] Lail M, Tanthana J, Coleman L. Non-aqueous solvent (NAS) CO_2 capture process. Energy Procedia. 2014;63:580–94.

[21] El Hadri N, Quang DV, Goetheer ELV, Abu Zahra MRM. Aqueous amine solution characterization for post-combustion CO_2 capture process. Appl Energy. 2017;185:1433–49.

[22] Zhao B, Sun Y, Yuan Y, Gao J, Wang S, Zhuo Y, et al. Study on corrosion in CO_2 chemical absorption process using amine solution. Energy Procedia. 2011;4:93–100.

[23] Barzagli F, Lai S, Mani F. Novel non-aqueous amine solvents for reversible CO_2 capture. Energy Procedia. 2014;63:1795–804.

[24] Guo H, Li C, Shi X, Li H, Shen S. Nonaqueous amine-based absorbents for energy efficient CO_2 capture. Appl Energy. 2019;239:725–34.

[25] Li X, Ding Y, Guo L, Liao Q, Zhu X, Wang H. Non-aqueous energy-efficient absorbents for CO_2 capture based on porous silica nanospheres impregnated with amine. Energy. 2019;171:109–19.

[26] Lv B, Guo B, Zhou Z, Jing G. Mechanisms of CO_2 capture into monoethanolamine solution with different CO_2 loading during the absorption/desorption processes. Environ Sci Technol. 2015;49(17):10728–35.

[27] Tao M, Gao J, Zhang P, Zhang W, Liu Q, He Y, et al. Biogas upgrading by capturing CO_2 in non-aqueous phase-changing diamine solutions. Energy Fuels. 2017;31(6):6298–304.

[28] Aghel B, Janati S, Wongwises S, Shadloo MS. Review on CO_2 capture by blended amine solutions. Int J Greenh Gas Control. 2022;119:103715.

[29] Hu X, Huang J, He X, Luo Q, Li C, Zhou C, et al. Analyzing the potential benefits of trio-amine systems for enhancing the CO_2 desorption processes. Fuel. 2022;316:123216.

[30] Pellegrini LA, Gilardi M, Giudici F, Spatolisano E. New solvents for CO_2 and H_2S removal from gaseous streams. Energies. 2021;14:6687.

[31] Yu YS, Lu HF, Zhang TT, Zhang ZX, Wang GX, Rudolph V. Determining the performance of an efficient nonaqueous CO_2 capture process at desorption temperatures below 373 K. Ind Eng Chem Res. 2013;52(35):12622–34.

[32] Yu CH, Wu TW, Tan CS. CO_2 capture by piperazine mixed with non-aqueous solvent diethylene glycol in a rotating packed bed. Int J Greenh Gas Control. 2013;19:503–9.

[33] Im J, Hong SY, Cheon Y, Lee J, Lee JS, Kim HS, et al. Steric hindrance-induced zwitterionic carbonates from alkanolamines and CO_2: highly efficient CO_2 absorbents. Energy Environ Sci. 2011;4(10):4284–9.

[34] Chen S, Chen S, Fei X, Zhang Y, Qin L. Solubility and characterization of CO_2 in 40 mass % N-Ethylmonoethanolamine

solutions: Explorations for an efficient nonaqueous solution. Ind Eng Chem Res. 2015;54(29):7212–8.

[35] Xiao M, Liu H, Gao H, Olson W, Liang Z. CO$_2$ capture with hybrid absorbents of low viscosity imidazolium-based ionic liquids and amine. Appl Energy. 2019;235:311–9.

[36] Cao J, Yang M, Cao F, Wang J, Su E. Tailor-made hydrophobic deep eutectic solvents for cleaner extraction of polyprenyl acetates from Ginkgo biloba leaves. J Clean Prod. 2017;152:399–405.

[37] Niedermaier I, Bahlmann M, Papp C, Kolbeck C, Wei W, Krick CS, et al. Carbon dioxide capture by an amine functionalized ionic liquid: fundamental differences of surface and bulk behavior. J Am Chem Soc. 2014;136(1):436–41.

[38] Raja Shahrom MS, Wilfred CD, MacFarlane DR, Vijayraghavan R, Chong FK. Amino acid based poly(ionic liquid) materials for CO$_2$ capture: effect of anion. J Mol Liq. 2019;276:644–52.

[39] Wang C, Luo H, Luo X, Li H, Dai S. Equimolar CO$_2$ capture by imidazolium-based ionic liquids and superbase systems. Green Chem. 2010;12(11):2019–23.

[40] Luo X, Guo Y, Ding F, Zhao H, Cui G, Li H, et al. Significant improvements in CO$_2$ capture by pyridine-containing anion-functionalized ionic liquids through multiple-site cooperative interactions. Angew Chem. 2014;53(27):7053–7.

[41] Gutowski KE, Maginn EJ. Amine-functionalized task-specific ionic liquids: a mechanistic explanation for the dramatic increase in viscosity upon complexation with CO$_2$ from molecular simulation. J Am Chem Soc. 2008;130(44):14690–704.

[42] Trivedi TJ, Lee JH, Lee HJ, Jeong YK, Choi JW. Deep eutectic solvents as attractive media for CO$_2$ capture. Green Chem. 2016;18(9):2834–42.

[43] Uma Maheswari A, Palanivelu K. Carbon dioxide capture and utilization by alkanolamines in deep eutectic solvent medium. Ind Eng Chem Res. 2015;54(45):11383–92.

[44] Zhang Q, De Oliveira Vigier K, Royer S, Jérôme F. Deep eutectic solvents: syntheses, properties and applications. Chem Soc Rev. 2012;41(21):7108–46.

[45] Li K, Yu H, Tade M, Feron P, Yu J, Wang S. Process modeling of an advanced NH$_3$ abatement and recycling technology in the ammonia-based CO$_2$ capture process. Environ Sci Technol. 2014;48(12):7179–86.

[46] Abu-Zahra MRM, Schneiders LHJ, Niederer JPM, Feron PHM, Versteeg GF. CO$_2$ capture from power plants: Part I. Int J Greenh Gas Control. 2007;1:37–46.

[47] Li BH, Zhang N, Smith R. Simulation and analysis of CO$_2$ capture process with aqueous monoethanolamine solution. Appl Energy. 2016;161:707–17.

[48] Zhang Q, Turton R, Bhattacharyya D. Development of model and model-predictive control of an MEA-based post combustion CO$_2$ capture process. Ind Eng Chem Res. 2016;55(5):1292–308.

[49] Mofarahi M, Khojasteh Y, Khaledi H, Farahnak A. Design of CO$_2$ absorption plant for recovery of CO$_2$ from flue gases of gas turbine. Energy. 2008;33(8):1311–9.

[50] Oh SY, Binns M, Cho H, Kim JK. Energy minimization of MEA-based CO$_2$ capture process. Appl Energy. 2016;169:353–62.

[51] Zhang W, Chen J, Luo X, Wang M. Modelling and process analysis of post-combustion carbon capture with the blend of 2-amino-2-methyl-1-propanol and piperazine. Int J Greenh Gas Control. 2017;63:37–46.

[52] Ali E, Hadj-Kali MK, Mulyono S, Alnashef I, Fakeeha A, Mjalli F, et al. Solubility of CO$_2$ in deep eutectic solvents: Experiments and modelling using the Peng–Robinson equation of state. Chem Eng Res Des. 2014;92(10):1898–906.

[53] Ali E, Hadj-Kali MK, Mulyono S, Alnashef I. Analysis of operating conditions for CO$_2$ capturing process using deep eutectic solvents. Int J Greenh Gas Control. 2016;47:342–50.

[54] Kohl AL, Nielsen R. Gas purification. 5th edn. Houston, Texas, USA: Gulf Professional Publishing; 1997.

[55] Smith JM, Van Ness HC, Abbott MM. Introduction to chemical engineering thermodynamics. 8th Edn. Boston, USA: McGraw-Hill; 2018.

[56] Wall G. Life cycle exergy analysis of renewable energy systems. Open Renew Energy J. 2011;4(1):1–6.

[57] Kutz M. Mechanical engineers' handbook, 1. Materials and engineering mechanics. New Jersey, USA: John Wiley & Sons; 2015.

[58] Srivathsan G. Modeling of fluid flow in spiral wound reverse osmosis membranes. Ph.D. dissertation. USA: University of Minnesota; 2013.

[59] Øi LE. Aspen HYSYS simulation of CO$_2$ removal by amine absorption from a gas-based power plant. The 48th Scandinavian Conference on Simulation and Modeling (SIMS 2007). Linköping University Electronic Press; 2007. p. 73–81.

[60] Pan M, Aziz F, Li B, Perry S, Zhang N, Bulatov I, et al. Application of optimal design methodologies in retrofitting natural gas combined cycle power plants with CO$_2$ capture. Appl Energy. 2016;161:695–706.

[61] Nuchitprasittichai A, Cremaschi S. Optimization of CO$_2$ capture process with aqueous amines using response surface methodology. Comput Chem Eng. 2011;35(8):1521–31.

[62] Greer T. Modeling and simulation of post combustion CO$_2$ capturing. Master thesis. Norway: Telemark University College; 2008.

[63] Han C, Graves K, Neathery J, Liu K. Simulation of the energy consumption of CO$_2$ capture by aqueous monoethanolamine in pilot plant. Energy Environ Res. 2011;1(1):67.

[64] Kothandaraman A. Carbon dioxide capture by chemical absorption: a solvent comparison study. Ph.D. dissertation. USA: Massachusetts Institute of Technology; 2010.

[65] Abu-Zahra MRM, Niederer JPM, Feron PHM, Versteeg GF. CO$_2$ capture from power plants: Part II. Int J Greenh Gas Control. 2007;1(2):135–42.

[66] Øi LE, Kvam SHP. Comparison of energy consumption for different CO$_2$ absorption configurations using different simulation tools. Energy Procedia. 2014;63:1186–95.

[67] Rao AB, Rubin ES. Identifying cost-effective CO$_2$ control levels for amine-based CO$_2$ capture systems. Ind Eng Chem Res. 2006;45(8):2421–9.

[68] Li K, Cousins A, Yu H, Feron P, Tade M, Luo W, et al. Systematic study of aqueous monoethanolamine-based CO$_2$ capture process: Model development and process improvement. Energy Sci Eng. 2016;4(1):23–39.

Appendix

There are two degradation steps of MTPB-MEA indicated as point 1 and point 2. Point 1 with onset at ~150°C is likely associated with the degradation of amine functionality. Point 2 with an onset at ~400°C is likely associated with the degradation of bromide functionality. The MTPB-MEA DES is thermally stable up to 150°C.
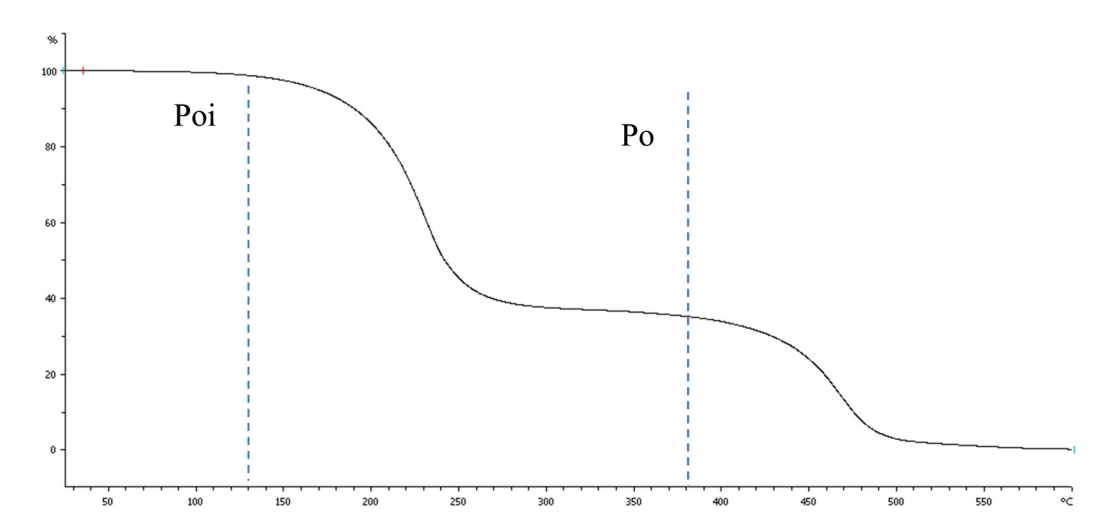

Figure A1: TGA of MTPB-MEA (1:6) deep eutectic solvent.

Table A1: physical properties of DES and MEA

Solvent	M_w (g·mol^{-1})	Density (kg·m^{-3})	C_p (J·g^{-1}·K^{-1})	Viscosity (cP)	T_n (°C)
DES	103.38	1,120	1.91	42.9	155
MEA	61.08	1,010	3.1*	17.9	170

* [62]

Table A2: Operating condition for conducting exergy and energy analysis

	DES					MEA
P_a (atm)	3	5	7	10	10 + ERD	1
T_a (°C)	25	25	25	25	25	40
T_s (°C)[c]	147	125	125	65	65	105[r1]
mH_2 (kg·kg CO_2^{-1})[c]	2.28	0.49	0.19	2.69	2.69	—
mH_3 (kg·kg CO_2^{-1})[c]	125.68	34.05	18.38	8.89	8.89	37.54
mH_4 (kg·kg CO_2^{-1})[c]	29.08	34.45	38.93	48.62	5.74	—
THE2$_i$ (°C)[a]	151	133	133	80	80	—
THE2$_o$ (°C)[a]	151	133	133	60	60	—
THE3$_i$ (°C)[a]	20	20	20	20	20	35
THE3$_o$ (°C)[a]	30	30	30	30	30	45
THE4$_i$ (°C)[a]	15	15	15	15	15	—
THE4$_o$ (°C)[a]	35	35	35	35	35	—
T_1 (°C)[c]	130	190	234	284	285	—
T_1i (°C)	–	–	–	–	217	–
T_2 (°C)[c]	143	121	122	62	62	–-
T_{lean} (°C)[a]	30	30	30	30	30	58
T_{st} (°C)[a]	—	—	—	—	—	100
T_{sd} (°C)[a]	—	—	—	—	—	75
T_{re} (°C)[r1]	—	—	—	—	—	120
Reboiler duty (MW·kg CO_2^{-1})[r2]	—	—	—	—	—	2.07
Condenser duty (MW·kg CO_2^{-1})[r2]	—	—	—	—	—	5.8

c – calculated, a – assumed arbitrary; r1: [66], r2: [49].

Table A3: Operating conditions for MEA process

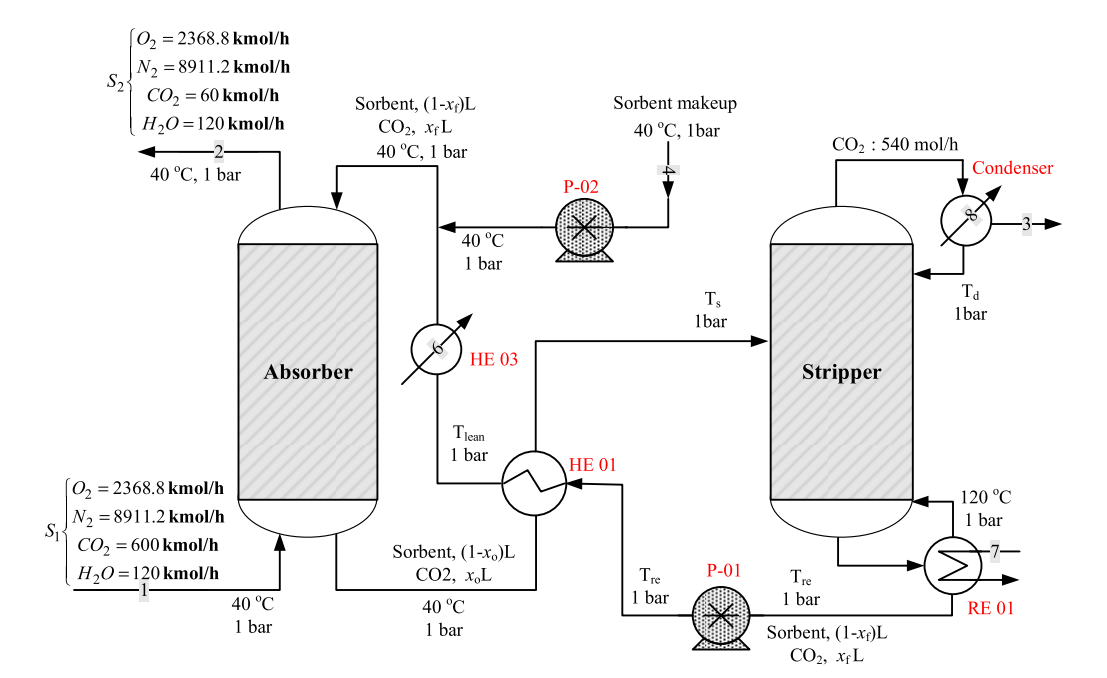| Parameter	[68]
G	2.62 kmol·h^{-1}
L	8.47 kmol·h^{-1}
Recovery rate	90%
CO_2 content in flue gas	1.4%
H_2O content in flue gas	11%
O_2 content in flue gas	0.094
N_2 content in flue gas	0.783
CO_2 mole fraction in rich sorbent	0.039
CO_2 mole fraction in lean sorbent	0.027
Stripper top temperature	NA
Stripper inlet temperature	112°C
Stripper bottom temperature	119.8°C
Reboiler duty	7.95 kW
Reboiler temperature	120°C
Absorber temperature	47°C
Absorber pressure	1.1 bar
Solvent circulation temperature	52°C
Condenser duty	2.77 kW

Figure A2: Schematic of CO_2 capture process using MEA.

Table A4: Design and operating condition from the process in Li et al. [68]

Parameter	DES			MEA
P_a (atm)	20	15	20 + ERD	1
T_a (°C)	47	47	47	47
T_s (°C)	60	107	60	120
mH_2 (kg·kg CO_2^{-1})	68.7	2.5	68.7	—
mH_3 (kg·kg CO_2^{-1})	138.5	138.4	138.5	282.3
mH_4 (kg·kg CO_2^{-1})	277.9	239.3	24.4	—
mCon (kg·kg CO_2^{-1})	—	—	—	119.4
mReS (kg·kg CO_2^{-1})	—	—	—	13.2
$THE2_i$ (°C)	70.6[a]	110[a]	70.6	—
$THE2_o$ (°C)	50.6[a]	110[a]	50.6	—
$THE3_i$ (°C)	20[a]	20[a]	42	42[a]
$THE3_o$ (°C)	30[a]	30[a]	52	52[a]
$THE4_i$ (°C)	15[a]	15[a]	37	—
$THE4_o$ (°C)	35[a]	35[a]	57	—
T_1 (°C)	443.6	392.5	79.5	—
T_2 (°C)	55.6	102.9	55.6	—
T_{lean} (°C)	30	30	30	56.4
T_{si} (°C)	—	—	—	112
T_{sb} (°C)	—	—	—	119
T_{st} (°C)	—	—	—	28a
T_{sd} (°C)	—	—	—	18

[a] Assumed arbitrary.